New ternary superconducting compound $LaRu_2As_2$: Physical properties from density functional theory calculations

M A Hadi[1,†], M S Ali[2], S H Naqib[1], and A K M A Islam[1,3]

[1] *Department of Physics, University of Rajshahi, Rajshahi* 6205, *Bangladesh*
[2] *Department of Physics, Pabna University of Science and Technology, Pabna* 6600, *Bangladesh*
[3] *International Islamic University Chittagong, Chittagong* 4203, *Bangladesh*

(Received 3 November 2016; revised manuscript received 13 December 2016; published online 13 February 2017)

In this paper, we perform the density functional theory (DFT) -based calculations by the first-principles pseudopotential method to investigate the physical properties of the newly discovered superconductor $LaRu_2As_2$ for the first time. The optimized structural parameters are in good agreement with the experimental results. The calculated independent elastic constants ensure the mechanical stability of the compound. The calculated Cauchy pressure, Pugh's ratio as well as Poisson's ratio indicate that $LaRu_2As_2$ should behave as a ductile material. Due to low Debye temperature, $LaRu_2As_2$ may be used as a thermal barrier coating (TBC) material. The new compound should exhibit metallic nature as its valence bands overlap considerably with the conduction bands. $LaRu_2As_2$ is expected to be a soft material and easily machinable because of its low hardness value of 6.8 GPa. The multi-band nature is observed in the calculated Fermi surface. A highly anisotropic combination of ionic, covalent and metallic interactions is expected to be in accordance with charge density calculation.

Keywords: new superconductor $LaRu_2As_2$, density functional theory (DFT) calculations, mechanical properties, electronic features

PACS: 71.20.Be, 71.15.Mb, 62.20.–x, 71.20.–b **DOI:** 10.1088/1674-1056/26/3/037103

1. Introduction

A great variety of compounds with RT_2X_2 stoichiometry possess the body-centered tetragonal $ThCr_2Si_2$-type structure (space group $I4/mmm$, No. 139).[1] In this stoichiometry, R is symbolized for a rare earth, alkaline earth or alkali element, T refers to a transition metal, and X represents p-metal atoms, namely B, P, Si, As, or Ge. This large family includes more than 700 members of 122-type intermetallics (so-called 122 phases) and exhibits an outstanding collection of physical and chemical properties.[2] The structure of RT_2X_2 stoichiometry offers an innate multilayer system in which the planes of R ions are taken apart from T metallic layers by X atomic sheets, comprising R–X–T–X–R stacking of individual basal planes along the c axis. The $ThCr_2Si_2$-type structure exhibits a strong uniaxial anisotropy with keeping c axis as an anisotropy axis. In other words, the layer of edge sharing TX_4 tetrahedron that is parallel to the ab plane and separated by the basal plane of R atoms characterizes the structure of RT_2X_2. In this structure, the R atomic sheets separate into two adjacent $[T_2X_2]$ blocks. In sequence, T ions inside $[T_2X_2]$ blocks build up a square lattice pressed between two X sheets shifted in order that each T is enclosed by a distorted X tetrahedron TX_4. A wide range of variation occurs in the interlayer distance between X atoms when either R or T is changed for a particular p-metal atom.[2,3]

This group of materials has attracted a lot of attention in recent years because of the discovery of high-temperature superconductivity in iron arsenide AFe_2As_2 (A = K, Ca, Sr, Ba, etc.).[4,5] As Ru lies in the same group together with Fe in the periodic table, the superconductivity in the level of iron arsenide is anticipated for Ru-related compounds, and several studies have been devoted to these materials.[6–10] Motivated by this, Guo *et al.*[11] have recently synthesized the polycrystalline samples of $ThCr_2Si_2$-type $LaRu_2As_2$ and reported the bulk superconductivity in $LaRu_2As_2$. Their temperature-dependent resistivity measurement ensures a superconducting transition of $LaRu_2As_2$ with an onset T_c of 7.8 K. This measurement also estimates the upper critical field $\mu_0 H_{c2}(0)$ at zero temperature and obtains a value of 1.6 T. Further, direct current (DC) magnetic susceptibility measurement detects a bulk superconducting Meissner transition at 7.0 K, and the isothermal magnetization measurement signifies that $LaRu_2As_2$ is a type-II superconductor. Surprisingly, $LaRu_2As_2$ has the highest transition temperature T_c among the iron-free transition metal pnictides with the $ThCr_2Si_2$-type crystal structure.

In this paper, the study of $LaRu_2As_2$ is carried out via the ground state electronic structure calculations by using the plane-wave pseudopotential approach within the density functional formalism. The aim of the present paper is to investigate the ground state properties including structural, elastic, electronic, and bonding characters of the newly discovered 122 phase compound by calculating its total energy in an optimized volume. To the best of our knowledge, this is the first *ab initio*

†Corresponding author. E-mail: hadipab@gmail.com

© 2017 Chinese Physical Society and IOP Publishing Ltd

calculation completed on this new superconductor $LaRu_2As_2$.

The rest of this paper is divided into three sections. In Section 2, a brief description of the method of computation used in this study is presented. The results obtained for the structural, elastic, electronic, and bonding properties of $LaRu_2As_2$ are analyzed in Section 3. Finally, Section 4 consists of the main conclusions of the present work.

2. Method of calculation

The approach used to investigate the physical properties of $LaRu_2As_2$ as implemented in the Cambridge Serial Total Energy Package (CASTEP) code[12] is as follows: a set of Kohn–Sham equations are solved by means of the plane-wave pseudopotential method[13] within the strong electron ensemble density functional theory (DFT).[14] Exchange and correlation energies are described by a nonlocal correction for local density approximation (LDA) in the form of generalized gradient approximation (GGA).[15] The wavefunctions are allowed to expand in a plane wave basis set by following the periodic boundary conditions and Bloch's theorem.[16] The electron–ion potential is treated by means of first-principles pseudopotentials within Vanderbilt-type ultrasoft formulation.[17] Broyden–Fletcher–Goldfarb–Shanno (BFGS) energy minimization technique[18] best for crystalline materials is used to find, self-consistently, the electronic wavefunctions and consequent charge density. In addition, the density mixing[19,20] scheme is employed. For k-points sampling integration over the first Brillouin, the Monkhorst–Pack scheme[21] is used. The parameters that are chosen for the present calculations are as follows: energy cutoff is 500 eV (340 eV for elastic property calculations), k-point mesh is $16 \times 16 \times 7$, the difference in total energy per atom is within 5×10^{-6} eV, maximum ionic Hellmann–Feynman force is within 0.01 eV/Å, maximum stress is within 0.02 GPa, and maximum ionic displacement is within 5×10^{-4} Å.

3. Physical properties

In this section the investigated physical properties of the 122 phase superconductor $LaRu_2As_2$ are presented and analyzed; among them are the structural and elastic properties, Debye temperature, band structure and density of states (DOS), and then Mulliken population and Vickers hardness and the electron charge density as well as Fermi surface of $LaRu_2As_2$ under zero pressure.

3.1. Structural properties

The body centered tetragonal $LaRu_2As_2$ structure crystallizes with space group $I4/mmm$ (No. 139) as shown in Fig. 1. Each atomic species in this crystal occupies only one crystallographic position and only one internal parameter z_X settles the relative position of As inside the unit cell. There are two formula units in each unit cell. The 2a, 4d, and 4e atomic positions are inhabited by the La, Ru, and As atoms, respectively. The negatively charged $[Ru_2As_2]$ blocks and positively charged La layers take positions by turns along the c-direction and form the crystal structure. The optimized lattice constants and z_X parameter of $LaRu_2As_2$ are given in Table 1 along with those obtained for some other 122 phase compounds. The computed lattice parameters accord well with the measured values.[11] Moreover, the calculated structural parameters are slightly larger ($a \sim 0.23\%$, $c \sim 2.94\%$, and $V \sim 3.41\%$) than the experimental values, which is a general trend inherent to GGA calculations.

Table 1. Structural properties of $LaRu_2As_2$ in comparison with those for the related $ThCr_2Si_2$-type compounds.

Compounds	a/Å	c/Å	V/Å^3	c/a	z_X	References
$LaRu_2As_2$	4.1923	10.9014	191.59	2.6003	0.3641	This
	4.1826	10.5903	185.27	2.5320	–	[11]
$BaRu_2As_2$	4.1925	12.3136	216.44	2.9371	0.3510	[22]
	4.1525	12.2504	211.24	2.9501	0.3527	[23]
$SrRu_2As_2$	4.2068	11.2903	199.81	2.6838	0.3591	[22]
	4.1713	11.1845	194.61	2.6813	0.3612	[23]

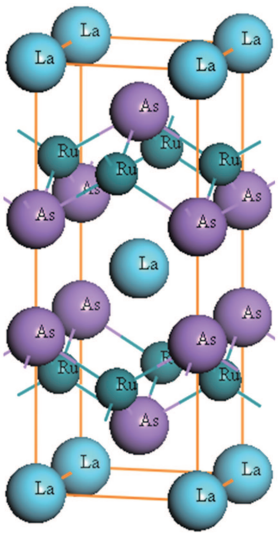


Fig. 1. (color online) Crystal structure of new 122 phase superconductor $LaRu_2As_2$.

3.2. Elastic properties

The mechanical behavior of solids can be described successfully by the elastic constants that are related to the material's response to an applied stress. The finite strain theory assigned in CASTEP code is well established for calculating the elastic constants successfully for a range of materials including metallic systems.[24] In this method, a given uniform deformation ε_j is used and then the resulting stress σ_i is calculated. By choosing an appropriate functional deformation, elastic constants are then evaluated by solving the linear equation, $\sigma_i = C_{ij}\varepsilon_j$.

The well-established Voight–Reuss–Hill (VRH) approximations validated in many metallic and insulating materials[25–27] are used to calculate the polycrystalline bulk elastic properties, namely, bulk modulus B and shear modulus G from calculated C_{ij}. Further, the equations $Y = (9GB)/(3B+G)$ and $v = (3B-2G)/(6B+2G)$ are employed to determine the Young's modulus Y and Poisson's ratio v, respectively.

The values obtained for single crystal elastic constants (C_{11}, C_{12}, C_{13}, C_{33}, C_{44}, and C_{66}) and bulk elastic properties (B, G, Y, B/G, and v) of tetragonal crystal system $LaRu_2As_2$ are listed in Table 2 along with the results found in the literature for La-based isostructural compounds.[28] The mechanical stability conditions for tetragonal crystals[29] are as follows: $C_{11} > 0$, $C_{33} > 0$, $C_{44} > 0$, $C_{66} > 0$, $C_{11} - C_{12} > 0$, $C_{11} + C_{33} - 2C_{13} > 0$, and $2(C_{11} + C_{12}) + C_{33} + 4C_{13} > 0$. These criteria are valid for the newly synthesized 122 phase, indicating the mechanical stability of the compound. The elastic constants C_{11} and C_{33} explain the linear compression resistances along the a- and c-directions, respectively. It is evident that the obtained elastic constants C_{11} and C_{33} are very large in comparison to other elastic constants, implying that the $LaRu_2As_2$ crystal should be very incompressible under uniaxial stress along both a- and c-directions. Again, the elastic constant C_{11} is much larger than C_{33}, meaning that the incompressibility along the a-direction should be much higher than that along the c-direction. In fact, the bonds aligned to the a-axis contribute a dominating effect on C_{11}, making it much larger than C_{33}. Since $C_{11} + C_{12} > C_{33}$, the bonding in the (001) plane should exhibit more elastic rigidity than that along the c-axis, and the elastic tensile modulus should be higher on the (001) plane than that along the c-axis. The elastic constant C_{44} indicates the ability to resist the shear distortion in (100) plane, whereas the elastic constant C_{66} is correlated with the resistance to shear in the $\langle 110 \rangle$ direction.[30] Since $C_{66} > C_{44}$, the new compound should be more competent to resist the shear distortion in the $\langle 110 \rangle$ direction than in the (100) plane. The shear anisotropy factor A, defined as $A = 2C_{66}/(C_{11} - C_{12})$ is 1.24, signifying that the shear elastic properties of the (001) plane in $LaRu_2As_2$ depend on the shear directions significantly.

The concept of failure mode, i.e., ductile or brittle nature, of materials is important in the study of mechanical behaviors of solids. A material can be either brittle or ductile in most practical situations. To quantify the failure state of solids, Cauchy pressure, and Pugh and Poisson's ratios are used as powerful tools. A brittle material changes its volume easily and a ductile material can be easily distorted under the action of external loads. The Cauchy pressure[31] defined as $(C_{12} - C_{44})$ identifies a solid as either a brittle or ductile one. When Cauchy pressure is positive (negative), the material is prone to being ductile (brittle). In accordance with Pugh's ratio,[32] the high (low) B/G value signifies the ductile (brittle) nature of the materials. The threshold value of B/G is found to be 1.75, which separates the ductile materials from brittle ones. Frantsevich *et al.*[33] separated the ductile materials from brittle materials in terms of Poisson's ratio. This rule proposes $v \sim 0.26$ as the border line that separates the brittle and ductile materials. A material having the Poisson's ratio greater than 0.26 will be ductile, otherwise the material will be brittle.

The Cauchy pressure $(C_{12} - C_{44})$ of $LaRu_2As_2$ is positive, its Pugh's ratio B/G is 1.79 which is greater than 1.75 and its Poisson's ratio v is 0.265 which is greater than 0.26. As a result, the compound $LaRu_2As_2$ should behave as a ductile material. It should be mentioned that there are some papers[34–37] in which $B/G = 2.0$ ($G/B = 0.5$) and $v \sim 0.33$ are used as critical values for separating the brittle materials from ductile ones. On the other hand, many authors[38–44] used the values presented in this paper to judge the brittle/ductile nature of the materials. In fact, Vaitheeswaran *et al.*[39] preferred $B/G = 1.75$ as threshold value for defining the brittle/ductile nature of the materials and showed that Pugh's critical value corresponds to $v = 0.26$ as the border line between the ductile and brittle materials. These criteria are frequently used to identify the brittle material from ductile ones.

Table 2. Single crystal elastic constants C_{ij}, polycrystalline bulk modulus B, shear modulus G, and Young's modulus Y, in GPa, Pugh's ratio G/B, and Poisson's ratio v of $LaRu_2As_2$.

Compounds	C_{11}	C_{12}	C_{13}	C_{33}	C_{44}	C_{66}	B	G	Y	B/G	v	A	Ref.
$LaRu_2As_2$	244	86	82	113	62	98	113	63	159	1.79	0.265	1.24	This
$LaNi_2Ge_2$	152	87	40	126	87	90	62	74	159	0.84	0.073	2.77	[28]
$LaNi_2P_2$	202	116	15	102	116	97	62	93	186	0.67	0.002	2.26	[28]

For describing the elastic behaviors of solids, bulk and shear moduli are two important parameters. Fracture and plastic deformation are two essential issues related to solid materials. Bulk modulus B measures the resistance to fracture and shear modulus G evaluates the resistance to plastic deformation of polycrystalline materials.[45] From dislocation theory[46] it is known that a weak relationship is observed between bulk modulus and hardness. On the contrary, a good relationship exists between hardness and shear modulus.[47] Certainly, the hardness is less susceptible to the bulk modulus than the shear modulus. Therefore, as can be seen from Table 2, the hardness of $LaRu_2As_2$ is expected to be small and

$LaRu_2As_2$ should be soft and easily machinable.

Many important issues related to physical properties of solids can be addressed with Young's modulus. The resistance in opposition to longitudinal tension can be estimated with Young's modulus Y. The Young's modulus also manipulates the thermal shock resistance of solids because of having the relation between critical thermal shock coefficient R and Y. In fact, the critical thermal shock coefficient R is found to be changed in inverse proportion to the Young's modulus Y.[48] The larger the R value, the better the thermal shock resistance. The thermal shock resistance is a fundamental parameter for thermal barrier coating (TBC) material selection. In comparison with a promising thermal barrier coating material $Y_4Al_2O_9$,[49] the small Y value of $LaRu_2As_2$ signifies that it should have a reasonable resistance to thermal shock.

3.3. Debye temperature

Debye temperature θ_D is a distinctive temperature of crystals at which the highest-frequency mode (and hence all modes) of vibration is excited. It controls many physical properties of materials and is used to make a division between high- and low-temperature regions for a solid. To distinguish the classical and quantum behavior of phonons, the Debye temperature also defines a border line between them. When the temperature T of a solid is elevated over θ_D, each mode of vibrations is expected to be associated with an energy equal to k_BT. At $T < \theta_D$, all high-frequency modes seem to be in sleep. The vibrational excitations at low temperature are due to acoustic vibrations. The Debye temperature, θ_D, is determined by using one of the standard methods depending on the elastic moduli.[50] This method guides us in calculating the Debye temperature from the average sound velocity v_m by the following equation: $\theta_D = h/k_B[(3n/4\pi)N_A\rho/M]^{1/3}v_m$, where h refers to the Planck's constant, k_B represents the Boltzmann's constant, n is the number of atoms per formula unit, M is symbolized for molar mass, N_A is the Avogadro's number, and ρ denotes the mass density of solid. The average sound velocity within a material is obtained by $v_m = [1/3(1/v_l^3 + 2/v_t^3)]^{-1/3}$. Here v_l and v_t indicate the longitudinal and transverse sound velocities in crystalline solids and are expressed as $v_l = [(3B+4G)/3\rho]^{1/2}$ and $v_t = [G/\rho]^{1/2}$, respectively.

The Debye temperature in cooperation with longitudinal, transverse and average sound velocities calculated within the present formalism is listed in Table 3. The values of v_l, v_t, v_m, and θ_D found in Ref. [28] are calculated by using elastic moduli B and G within the Voigt approximation. Here we convert these values into aggregate values using Hill approximations.[27] As a rule of thumb, a lower Debye temperature involves a lower phonon thermal conductivity. The examined phase $LaRu_2As_2$ has the lower Debye temperature than the other two isostructural compounds as well as a candidate material for thermal barrier coating $Y_4Al_2O_9$[49] and hence has a lower thermal conductivity. Accordingly, $LaRu_2As_2$ should have opportunity to be used as a thermal barrier coating (TBC) material.

Table 3. Calculated values of density (ρ in gm/cm^3), longitudinal, transverse, and average sound velocities (v_l, v_t, and v_m in km/s) and Debye temperature (θ_D in K) of $LaRu_2As_2$.

Compounds	ρ	v_l	v_t	v_m	θ_D	Refs.
$LaRu_2As_2$	8.799	4.731	2.676	2.976	335	This
$LaNi_2Ge_2$	7.685	4.572	3.103	3.384	389	[28]
$LaNi_2P_2$	6.853	5.210	3.684	3.994	478	[28]

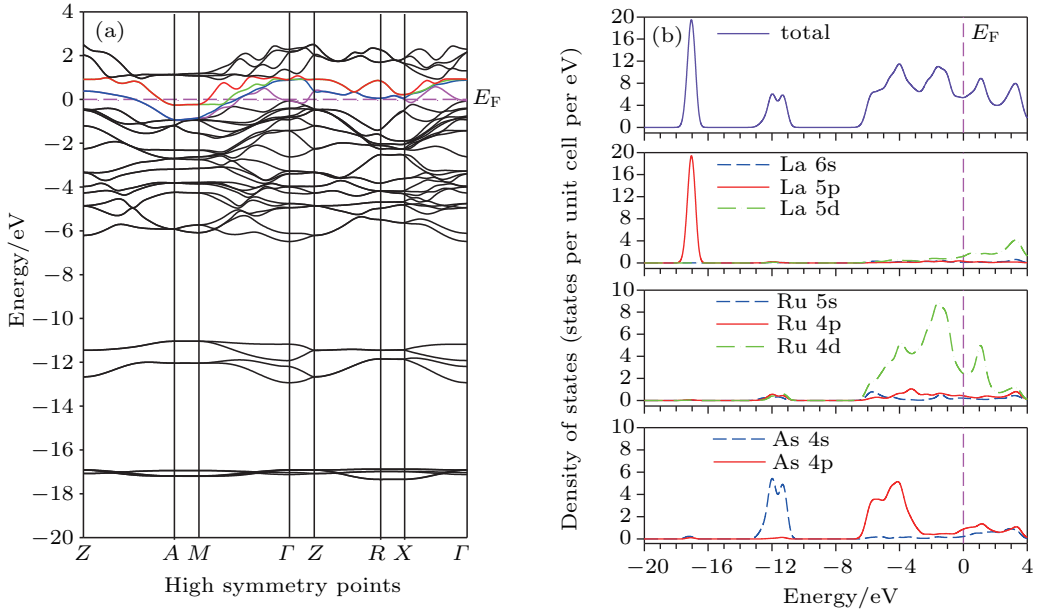


Fig. 2. (color online) Electronic structures of $LaRu_2As_2$, showing (a) electronic band structure, (b) total and partial densities of states.

3.4. Band structure and DOS

Understanding of electronic features (band structure, DOS, etc) is important to explain many physical phenomena, namely optical spectra and transport properties of solids. The full picture of energy bands and band gaps of a solid is known as electronic band structure or simply band structure. Actually, in solid-state and condensed matter physics, the band structure defines certain ranges of energy, which are allowed for electrons within a solid, and the ranges of energy, which are not allowed for any electrons. The number of bands indicates the available number of atomic orbitals in the unit cell. The calculated energy band structure with high symmetry points in the first Brillouin zone using equilibrium lattice parameters is shown in Fig. 2(a). The dashed line in the band structure corresponds to the energy of the highest filled state. This energy level is known as Fermi level, $E_{\rm F}$. Depending on the position of $E_{\rm F}$, several important distinctions regarding the expected electrical conductivity of a material can be made. The Fermi level of the new 122 phase superconductor takes position just above the valence band maximum near the Γ point. The new compound should have metallic behaviors in nature since its valence bands cross the Fermi level and overlap noticeably with the conduction bands. In addition, no band gap is found in the Fermi level. The near-Fermi bands show a complicated 'mixed' character, combining the quasi-flat bands with a series of high-dispersive bands intersecting the Fermi level. The detailed features of band structure can be explained with the calculated total and partial densities of states.

The calculated total and partial densities of states are shown in Fig. 2(b), where the vertical broken line denotes the Fermi level, $E_{\rm F}$. At the left of the Fermi level, a deep valley is observed, which is known as pseudogap $E_{\rm p}$. The delocalized electrons occupy the levels above $E_{\rm p}$ and the materials containing such electrons turn into metalized ones. It is seen that the Fermi level of $LaRu_2As_2$ lies in a region of relatively low DOS. Consequently, the new compound should be stable in perspective of electronic features as stated in the free electron model.[51] The new 122 phase superconductor $LaRu_2As_2$ should exhibit metallic conductivity due to having finite value of total density of states (TDOS) at $E_{\rm F}$. The atom resolved partial DOS gives an insight into the electronic structure. Mainly Ru 4d states contribute to the DOS at the Fermi level along with little contribution from La 5d and As 2p states. At $E_{\rm F}$ the calculated TDOS has a value of 5.4 states per unit cell per eV. The large TDOS is a sign of high metallicity of the compound. The TDOS at the Fermi level is quite high compared with those of some other recently discovered ternary superconducting compounds.[52,53] This may be responsible for the higher superconducting transition temperature in $LaRu_2As_2$, than, for example, in ternary silicides.[54]

The lowest lying valence bands extended from -17.9 to -16.3 eV arise entirely from La 5p states. These valence bands are observed to be separated by a wide prohibited energy gap of ~ 3.3 eV from the next valence bands lying in an energy range from -13.0 eV to -10.6 eV. These valence bands are again separated by a forbidden energy gap of width 3.4 eV from the highest valence bands. The highest valence bands contain three visible peaks and broaden in an energy range from -6.6 eV to Fermi level. The left peak originates mainly from As 4p and Ru 4d states. The middle and highest peak are due to equal contribution from Ru 4d and As 4p states. The first peak near to Fermi level forms due to a contribution coming from Ru 4d states. In the energy range between -6.6 eV and the Fermi level, the covalent bonding between comprising elements is expected. This is due to the reason why the states are truly degenerate regarding angular momentum and lattice site. Because of the difference in the value of electronegativity among the constituent elements, few ionic interactions can be predicted within $LaRu_2As_2$ as well.

3.5. Mulliken population and Vickers hardness

The allocation of electrons in several fractional manners among the various parts of bonds can be explained by analyzing the Mulliken population. The overlap population provides a relation between covalency/ionicity of bonding and bond strength. Sanchez-Portal *et al.*[55] developed a method of analyzing the population in CASTEP code using a projection of the plane wave states onto a localized basis. The Mulliken scheme[56] is then applied to the population analysis of the resulting projected states. Analyzing the electronic structure calculations with linear combination of atomic orbital (LCAO) basis sets, this technique is used extensively. Using minimal basis Mulliken scheme[56,57] provides two fundamental quantities regarding atomic bond population, i.e., the effective charge and the bond order values between a pair of bonding atoms, which are expressed as

$$Q^*_\alpha = \sum_{i,\alpha} \sum_{n,\mathrm{occ}} \sum_{j,\beta} C^{*n}_{i\alpha} C^n_{j\beta} S_{i\alpha,j\beta},$$
$$\rho_{\alpha\beta} = \sum_{n,\mathrm{occ}} \sum_{i,j} C^{*n}_{i\alpha} C^n_{j\beta} S_{i\alpha,j\beta},$$

where i and j denote the orbital quantum numbers, n indicates the band index, $C^{*n}_{i\alpha}$ and $C^n_{j\beta}$ are the eigenvector coefficients of the wave function, and $S_{i\alpha,j\beta}$ is the overlap matrix between atoms α and β.

For understanding the bonding character in crystal systems the effective valence charge and Mulliken atomic population are two important parameters. The effective valence is the difference between the formal ionic charge and Mulliken charge on the anion species within a crystal. It measures the level of covalency/ionicity of a chemical bond. A chemical

bond becomes an ideal ionic bond if there are zero effective valences. In contrast, the positive effective valence indicates the presence of covalent bond and the high values signify the high level of covalency in chemical bonds. Table 4 lists the effective valences, which reveal the high degree of covalency in chemical bonds inside the new superconductor $LaRu_2As_2$. Table 5 gives the obtained bond overlap populations between nearest neighbors in this crystal. When the values of overlap population tend to be zero a trivial interaction occurs between the electronic populations of the two atoms. Actually, a weak bond occurs when small Mulliken population exists and such a bond makes a negligible contribution to material hardness. With a low overlap population a bond exhibits a high degree of ionicity, whereas with a high value the chemical bond possesses a high level of covalency. Positive and negative bond overlap populations lead to bonding and antibonding states, respectively.

Table 4. Population analyses of $LaRu_2As_2$.

Species	Mulliken atomic populations					Effective valence
	s	p	d	total	charge (e)	charge (e)
As	1.57	3.31	0.00	4.88	0.12	–
Ru	2.52	6.89	7.36	16.76	–0.76	3.76
La	1.92	6.01	1.77	9.71	1.29	1.71

Table 5. Calculated values of bond and total Vickers hardness H_v^μ, H_v (in GPa) of $LaRu_2As_2$ along with bond number n^μ, bond length d^μ (Å), bond volume v_b^μ (Å^3), and bond and metallic populations P^μ, $P^{\mu'}$.

Bond	n^μ	d^μ	P^μ	$P^{\mu'}$	v_b^μ	H_v^μ	H_v
Ru–Ru	2	2.96437	0.98	0. 11832	13.23	8.62	6.8
Ru–La	8	3.43822	1.47	0. 11832	20.64	6.44	

Hardness assesses the ability of a material to resist the plastic deformation. The magnitude of force acting on unit area and directing oppositely to plastic deformation, is used for estimating the hardness of a material. Gao[58] formulated an equation to determine the hardness values of non-metallic materials by using Mulliken population within first-principles approach. There is no direct relation between delocalized metallic bonding and hardness of material.[59] For this reason the above method cannot predict the hardness values of materials with partial metallic bonding. Gou *et al.*[60] developed an equation considering a correction for metallic bonding to calculate the bond hardness values of mixed metallic crystals as follows:

$$H_v^\mu = 740\left(P^\mu - P^{\mu'}\right)\left(v_b^\mu\right)^{-5/3},$$

where Mulliken overlap population of the μ-type bond is represented by P^μ, $P^{\mu'}$ is a symbol for metallic population and is calculated by using the unit cell volume V and the number of free electrons in a cell $n_{\text{free}} = \int_{E_P}^{E_F} N(E)\,\mathrm{d}E$ as $P^{\mu'} = n_{\text{free}}/V$, E_P represents the energy at pseudogap, and v_b^μ denotes the volume of a bond of μ-type, which can be calculated from the bond length d^μ of type μ and the number of bonds N_b^ν of type ν per unit volume through $v_b^\mu = (d^\mu)^3/\sum_\nu[(d^\mu)^3 N_b^\nu]$.

For the complex multiband crystals the hardness can be calculated as a geometric average of all bond hardness values as follows:[61,62]

$$H_V = \left[\prod^{\mu}(H_v^\mu)^{n^\mu}\right]^{1/\Sigma n^\mu},$$

where n^μ represents the number of $\mu-$type bonds, which constitute the real multiband crystals. The evaluated Vickers hardness in consideration of positive and reasonable populations between nearest neighbors for the new compound $LaRu_2As_2$ is given in Table 5. The hardness value of 6.8 GPa for $LaRu_2As_2$ is much less than that of diamond (96 GPa), which is the hardest material known so far. Therefore, $LaRu_2As_2$ is a soft material and it should be easily machinable.

3.6. Electron charge density and Fermi surface

To visualize the nature of chemical bonding in $LaRu_2As_2$, the electron charge density distribution is calculated and the contour of electron charge density is presented in Fig. 3. On an adjacent scale, the blue and red colors signify the low and high electron densities, respectively. An atom with large electronegativity (electronic charge) exerts a pull on electron density towards itself.[63] Because of large difference in electronegativity and radius of atoms, the electronic charges around Ru (2.20) and As (2.18) are greater than that around La (1.10). The higher electronegativities of Ru and As exhibit strong accumulation of electronic charge while relatively low charge density indicates weak charge accumulation of La. A typical ionic picture based on standard oxidation states of atoms can help to explain the bonding nature of a compound. In $LaRu_2As_2$, the oxidation states of atoms are La^{2+}, Ru^{2+}, and As^{3-}. The sum of the oxidation numbers must be zero for a neutral compound such as $LaRu_2As_2$. In the $LaRu_2As_2$ structure, the $[Ru_2As_2]$ blocks are separated by La atomic sheets. The charge states of these sheets/blocks are $[La]^{2+}$ and $[(Ru^{2+})_2(As^{3-})2]^{2-}$. It can be said that a charge transfer will take place from $[La]^{2+}$ sheets to $[Ru_2As_2]^{2-}$ blocks. The existence of ionic bonds between Ru–As within $[Ru_2As_2]^{2-}$ blocks can be guessed from the balance between negative and positive charges at the positions of relevant atoms. From atom resolved DOS it is observed that the hybridization between Ru 4d and As 4p states leads to the formation of covalent Ru–As bonds. Moreover, metallic-type Ru–Ru bonds are expected to exist in $[Ru_2As_2]$ blocks due to overlapping of Ru 4d states near Fermi level (Fig. 2(b)). Surprisingly, no As–As bonds exist between two adjacent $[Ru_2As_2]$ blocks in $LaRu_2As_2$. But such bonds are found to be present in $(Ca/Ba)Fe_2As_2$ iron pnictides.[64] The possible reason for this contradiction may be explained as follows: the low strength of Fe–As bond in iron pnictide in comparison with Ru–As bonds in $LaRu_2As_2$ favors the formation of As–As bond in $(Ca/Ba)Fe_2As_2$. The above discussion reflects that the chemical bonding in $LaRu_2As_2$ can be described as a highly anisotropic combination of ionic, covalent and metallic interactions.

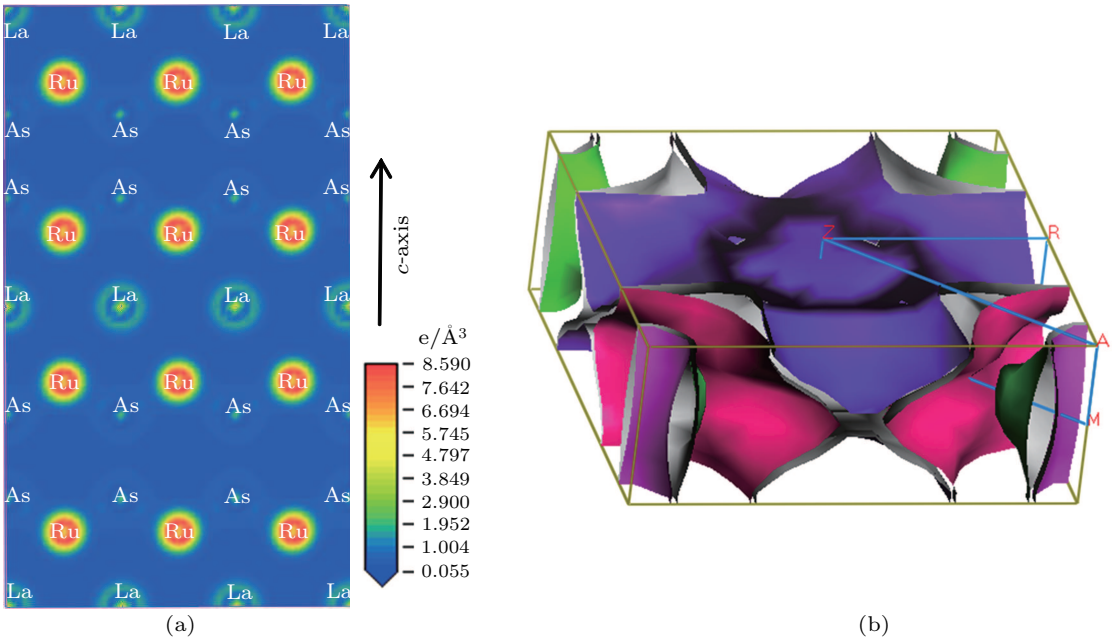


Fig. 3. (color online) Charge density (a) and Fermi surface (b) of $LaRu_2As_2$.

The Fermi surface topology is calculated, which is presented in Fig. 3(b). As is observed, the near-Fermi surface band picture has a complicated 'mixed' character: the quasi-flat band and the high-dispersive band intersect the Fermi level simultaneously. These features concede a multi-sheet Fermi surface consisting of two quasi-two-dimensional electron-like sheets in the corners of the Brillouin zone. The nearest sheet is also parallel to *A*–*M* direction and the distant sheet is half-folded and intersected at the centre of the sheet by the Γ–*M* line. Between these two sheets a concave sheet appears and the Γ–*M* line serves as the axis of this three-dimensional sheet. The central electron-like sheet is very complicated and has four half-tube shaped wings cutting along its own axis. These four wings form a red-cross shape keeping each arm along the *Z*–*R* direction. The existence of the multiband nature suggests that the new compound $LaRu_2As_2$ could be a class of multiple-gap superconductor.

3.7. Electron–phonon coupling constant

Accurate value of electron–phonon coupling constant (λ) is important for evaluating the superconducting transition temperature T_c. The method assigned to QUANTUM ESPRESSO program[65] can accurately compute the λ value directly. We stress that a double-delta function integration over a dense net of electron and phonon vectors (k and q) is required to compute the electron–phonon coupling constant with significant computational resources. Moreover, this method is more complicated for a crystal system containing many atoms in its unit cell like $LaRu_2As_2$. All of these prohibit us from carrying on with this method. We have an alternative method in which the equation $1+\lambda = 3\gamma/[2\pi^2 k_B^2 N(E_F)]$ provides the electron–phonon coupling constant.[66] However, in the present situation we have no experimental values for electronic specific-heat coefficient γ and theoretically calculated value yields a lower value of λ.[67] So, we have only one indirect method based on McMillan's equation to calculate the value of λ as follows:

$$\lambda = \frac{1.04+\mu \ln\left(\frac{\theta_D}{1.45T_c}\right)}{(1-0.62\mu^*)\ln\left(\frac{\theta_D}{1.45T_c}\right)-1.04}.$$

The repulsive Coulomb potential μ^* is assigned to a value in a range of 0.10–0.15 and the choice of μ^* is fairly arbitrary. Using known $T_c = 7.8$ K[11] with our calculated Debye temperature $\theta_D = 335$ K in McMillan's equation, we have $\lambda = 0.64$ and 0.76 for $\mu^* = 0.1$ and 0.15, respectively, which implies that $LaRu_2As_2$ should be a moderately coupled BCS superconductor.

4. Conclusions

DFT method is used within the first-principles pseudopotential method to calculate some physical properties of newly discovered superconductor $LaRu_2As_2$. The evaluated lattice constants show sound agreement with the experimental results. The obtained single crystal elastic constants obey the mechanical stability conditions for the new tetragonal system. The $LaRu_2As_2$ crystal shows high uniaxial elastic anisotropy. The newly synthesized compound is expected to resist the shear distortion in the $\langle 110 \rangle$ direction more strongly than in the (100) plane. Cauchy pressure, Poisson's ratio, and Pugh's ratio indicate that $LaRu_2As_2$ should be a ductile material. The relatively small Young's modulus indicates that $LaRu_2As_2$ should attain reasonable resistance to thermal shock. The low Debye

temperature also suggests that this compound should be favorable for use as a thermal barrier coating material. The calculated electronic structures reveal that the intra-atomic bonding in new 122 phase compound $LaRu_2As_2$ may be explained as a mixture of ionic, covalent and metallic interactions. The hardness value of 6.8 GPa implies that this material should be soft and easily machinable. The obtained Fermi surface exhibits the multi-band nature, suggesting that the new ternary compound $LaRu_2As_2$ could be a kind of multiple-gap superconductor. The calculated λ indicates the strong electron–phonon coupling in $LaRu_2As_2$. Very recently, we have noted that some *ab initio* calculations have been done on $LaRu_2As_2$ and $LaRu_2P_2$ compounds.[68] Some of the basic features of those calculations agree quite well with the ones presented in this paper. To conclude, we expect that this study will stimulate further experimental and theoretical research activities on the newly synthesized $LaRu_2As_2$ compound.

References

[1] Villars P and Calvert L D 1991 *Pearson's Handbook of Crystallographic Data for Intermetallic Phases*, 2nd ed, ASM International, Materials Park, OH
[2] Shameem Banu I B, Rajagopalan M, Mohammed Yousuf and Shenbagaraman P 1999 *J. Alloys Comp.* **288** 88
[3] Baran S, Bałanda M, Gondek L, Hoser A, Nenkov K, Penc B and Szytuła A 2010 *J. Alloys Comp.* **507** 16
[4] Rotter M, Tegel M and Johrendt D 2008 *Phys. Rev. Lett.* **101** 107006
[5] Sasmal K, Lorenz B L B, Guloy A M, Chen F, Xue Y Y and Chu C W 2008 *Phys. Rev. Lett.* **101** 107007
[6] Jeitschko W, Glaum R and Boonk L 1987 *J. Solid State Chem.* **69** 93
[7] Meisner G P 1981 *Physica B+C* **108** 763
[8] Shirotani I, Uchiumi T, Ohno K, *et al*. 1997 *Phys. Rev. B* **56** 7866
[9] Barz H, Ku H C, Meisner G P, *et al*. 1980 *Proc. Natl. Acad. Sci. USA* **77** 3132
[10] Meisner G P, Ku H C and Barz H 1983 *Mater. Res. Bull.* **18** 983
[11] Guo Q, Pan B J, Yu J, Ruan B B, Chen D Y, Wang X C, Mu Q G, Chen G F and Ren H A 2016 *Sci. Bull.* **61** 921
[12] Segall M, Probert M, Pickard C, Hasnip P, Clark S, Refson K, Yates J R and Payne M 2005 *Z. Kristallogr.* **220** 567
[13] Payne M C, Teter M P, Allan D C, Arias T A and Joannopoulos J D 1992 *Rev. Mod. Phys.* **64** 1045
[14] Marzari N, Vanderbilt D and Payne M C 1997 *Phys. Rev. Lett.* **79** 1337
[15] Perdew J P, Burke S and Ernzerhof M 1996 *Phys. Rev. Lett.* **77** 3865
[16] Bloch F 1928 *Z. Phys.* **52** 555
[17] Vanderbilt D 1990 *Phys. Rev. B* **41** 7892
[18] Fischer T H and Almlof J 1993 *J. Phys. Chem.* **96** 9768
[19] Kresse G and Furthmuller J 1996 *Phys. Rev. B* **54** 11169
[20] Alfe D 1999 *Comp. Phys. Commun.* **118** 31
[21] Monkhorst H J and Pack J D 1976 *Phys. Rev. B* **13** 5188
[22] Shein I R and Ivanovskii A L 2009 *Solid State Commun.* **149** 1860
[23] Nath R, Singh Y and Johnston D C 2009 *Phys. Rev. B* **79** 174513
[24] Murnaghan F D 1951 *Finite Deformation of an Elastic Solid* (New York: Wiley)
[25] Voigt W 1928 *Lehrbuch der Kristallphysik, Taubner* Leipzig
[26] Reuss A 1929 *Z. Angew, Math. Mech.* **9** 49
[27] Hill R 1952 *Proc. Phys. Soc. A* **65** 349
[28] Shein I R and Ivanovskii A L 2012 *Intermetallics* **26** 1
[29] Born M, Huang K and Lax M 1995 *Am. J. Phys.* **23** 474
[30] Koc H, Ozisik H, Deligöz E, Mamedov A M and Ozbay E 2014 *J. Mol. Model.* **20** 2180
[31] Pettifor D G 1992 *Mater. Sci. Technol.* **8** 345
[32] Pugh S F 1954 *Phil. Mag.* **45** 823
[33] Frantsevich I N, Voronov F F and Bokuta S A 1983 *Naukova Dumka, Kiev* 60–180
[34] Shein I R and Ivanovskii A L 2013 *Physica B* **410** 42
[35] Shein I R and Ivanovskii A L 2011 *Phys. Status Solidi B* **248** 228
[36] Shein I R and Ivanovskii A L 2010 *JETP Lett.* **91** 410
[37] Romero M and Escamilla R 2014 *Comp. Mater. Sci.* **81** 184
[38] Ravindran P, Fast L, Korzhavyi P A, Johansson, B, Wills J and Eriksson O 1998 *J. Appl. Phys.* **84** 4892
[39] Vaitheeswaran G, Kanchana V, Svane A and Delin A 2007 *J. Phys.: Conden. Matter* **19** 326214
[40] Aydin S and Özcan A 2010 *Turk. J. Phys.* **34** 1
[41] Dong B, Liu K, Zhou X L, Tan J, Mao X C and Chang J 2016 *Phys. Status Solidi B* **253** 527
[42] Li C, Wang C, Zhang F, Ma D, Wang B and Wu G 2008 *J. Phys. Chem. Solids* **78** 28
[43] Wu Z and Zhao E 2008 *J. Phys. Chem. Solids* **69** 2723
[44] Benayad N, Rached D, Khenata R, Litimein F, Reshak A H, Rabah M and Baltache H 2011 *Mod. Phys. Lett. B* **25** 747
[45] Varshney D and Shriya S 2013 *Phys. Chem. Minerals* **40** 521
[46] Westbrook J H and Conrad H 1973 *Conference Proceedings, The Science of Hardness Testing and Its Research Applications* (Metals Park, Ohio: ASM)
[47] Chung H Y, Weinberger M B, Yang J M, Tolbert S H and Kaner R B 2008 *Appl. Phys. Lett.* **92** 261904
[48] Wang X, Xiang H, Sum X, Liu J, Hou F and Zhou Y 2015 *J. Mater. Sci. Tech.* **31** 369
[49] Zhou Y, Xiang H, Lu X, Feng Z and Li Z 2015 *J. Adv. Ceram.* **4** 83
[50] Anderson O L 1963 *J. Phys. Chem. Solids* 24 909
[51] Nagel S and Tauc J 1975 *Phys. Rev. Lett.* **35** 380
[52] Hadi M A, Alam M A, Roknuzzaman M, Nasir M T, Islam A K M A and Naqib S H 2015 *Chin. Phys. B* **24** 117401
[53] Alam M A, Hadi M A, Nasir M T, Roknuzzaman M, Parvin F, Zilani M A K, Islam A K M A and Naqib S H 2016 *J. Supercond. Nov. Magn.* **29** 2503
[54] Hirai D, Kawakami R, Magdysyuk O, Dinnebier R E, Yaresko A and Takagi H 2014 *J. Phys. Soc. Jpn.* **83** 103703
[55] Sanchez-Portal D, Artacho E and Soler J M 1995 *Solid State Commun.* **95** 685
[56] Mulliken R S 1955 *J. Chem. Phys.* **23** 1833
[57] Ching W Y and Rulis P 2012 *Electronic Structure Methods for Complex Materials - The Orthogonalized Linear Combination of Atomic Orbitals* (Oxford Univ. Press)
[58] Gao F M 2006 *Phys. Rev. B* **73** 132104
[59] Westbrook J H and Conrad H 1973 *The Science of Hardness Testing and Its Research Applications* (ASM, Ohio)
[60] Gou H, Hou L, Zhang J and Gao F 2008 *Appl. Phys. Lett.* **92** 241901
[61] Szymański A and Szymański J M 1989 *Hardness Estimation of Minerals Rocks and Ceramic Materials*, 6th edn (Amsterdam: Elsevier)
[62] Glazov V M and Vigdorovid V N 1989 *Hardness of Metals* (Izd. Metellurgiya, Moskva)
[63] IUPAC 1997 *Compendium of Chemical Technology*, 2nd edn., 2006 Online corrected version
[64] Yildirim T 2009 *Phys. Rev. Lett.* **102** 037003
[65] Giannozzi P *et al*. 2009 *J. Phys. Condens. Matter* **21** 395502
[66] Lofland S E, Hettinger J D, Meehan T, Bryan A, Finkel P, Gupta S, Barsoum M W and Hug G 2006 *Phys. Rev. B* **74** 174501
[67] Savrasov S Y and Savrasov D Y 1996 *Phys. Rev. B* **54** 16487
[68] Rahaman M Z and Rahman M A 2016 arXiv:1609.08856